Int. J. Solids Structures Vol. 30, No. 2, pp. 249–261, 1993
Printed in Great Britain.

0020–7683/93 $5.00+.00

RATE DEPENDENT ELASTO–PLASTICITY OF HYBRID COMPOSITES IN COMPRESSION

YIREN XIA†
Department of Engineering Science, Oxford University, Parks Road, Oxford, OX1 3PJ, U.K.

(*Received* 2 *May* 1991; *in revised form* 13 *May* 1992)

Abstract—Rate dependent response of a polymer composite consisting of short glass fibres, rubber particles or glass beads and epoxy resin is studied theoretically, based on a micro-mechanics model. Various configurations of the system are simulated in order to obtain an optimal design in terms of high flow stress and low matrix deformation when loaded at matrix plastic strain rates ranging between 0.1 and 2000 s^{-1}.

1. INTRODUCTION

The mechanical behaviour of filled epoxy resins results from a complex interplay of properties of the constituent phases: resin and fillers. The principal relevant parameters are the volume fraction of filler, the particle size, the filler aspect ratio, the modulus and strength of the filler and the toughness of the matrix. It has been shown by Moloney *et al.* (1987) that by increasing filler volume fraction, tensile and compressive moduli, the flexural strength of a silica filled resin increase while the tensile strength drops first and then increases steadily. Changing the filler particle size at constant volume fraction does not have a significant influence on the modulus of the composite. Increasing the filler modulus increases the modulus of the resulting composite. The work of fracture increases with fibre length up to a critical aspect ratio (defined as the ratio of length to diameter of an inclusion), thereafter the energy drops when under tension. It is not clear how energy absorption capability changes with fibre length under compression. The main reason for incorporation of a secondary dispersed phase of rubber is to toughen the epoxy resin. According to Moloney *et al.* (1987), addition of rubber particles would dramatically increase the fracture toughness with only a small sacrifice in the modulus.

Tests carried out at Oxford (Xia *et al.*, 1991) on hybrid epoxy show that the composite exhibits a ductile behaviour with an ultimate compressive strain of up to 60%. Even loaded with low strain rate, rate effect occurs inevitably. This leads to a complex time dependent interaction between matrix and fillers. In the hybrid composites studied here, the aspect ratios are 1 for the spherical rubber particles or glass beads, and 5–15 for short glass fibres. It is assumed here that glass fibres, glass beads and rubber particles remain elastic whereas the resin undergoes elasto–plastic deformation. Therefore, apart from strain hardening effects, for the same value of strain, the stress is higher for higher strain rate and the amount in excess of the corresponding stress for a near-zero strain rate (quasi-static) is due to the visco–plastic effect. It is this overstress that is rate-dependent. In order to model this elasto–viscoplastic behaviour, a commonly used phenomenological constitutive relation is used and it simply reflects the experimental observations that the flow stress varies with strain, strain rate, etc. The Cowper–Symonds relation, claimed to be applicable to both metallic and non-metallic materials, is used.

The simulation of hybrid composites is facilitated by a micro-mechanics approach. It follows Mori-Tanaka's work which effectively is the Eshelby equivalent inclusion method but takes into account the interaction among inhomogeneities. The theory is superior to the classical rule of mixture and shear lag theories in that it gives better estimates for the stiffness and other mechanical properties of a composite with short fibres of small aspect ratio. A recent detailed description of the method was conducted by Withers *et al.* (1989).

† Now at Hibbitt, Karlsson & Sorensen, Inc., 1080 Main St., Pawtucket, RI 02860, U.S.A.

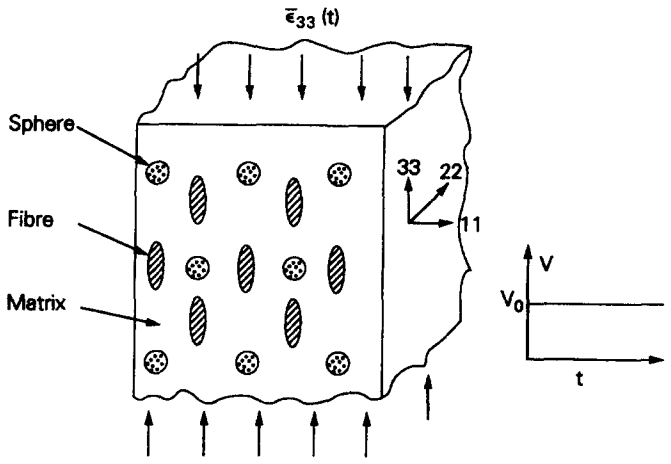

Fig. 1. A hybrid composite under impact ($\bar{\varepsilon}_{33} = -\ln(1-v_0 t/h_0)$).

The method has also been used by Taya and Chou (1981) and Taya and Arsenault (1989). The analysis here follows a somewhat similar form as Tandon and Weng (1988) and Weng (1988) but with three phases and rate dependency as its new features. Small strain assumption is made and so is the low concentration of inclusions. Christensen's review (1990) clearly pointed out that the method is applicable to composites of reasonably low concentration. Although the original theory of Tandon and Weng (1988) was intended for the rate independent plasticity, it is here used as a simple approximation for the rate dependent response.

The overall aim is to provide a picture of relations among various parameters. A hybrid epoxide body (see Fig. 1) pressed uniaxially under controlled velocity or displacement is studied.

2. THEORETICAL FORMULATIONS

The deformation theory is used, since in general constant velocity compression will generate monotonically increasing strain and strain rate. This will be proved later in the section of results. The total strain of the resin is the sum of elastic and plastic components. Its secant modulus, defined in an overall averaged sense, E_0^s decreases with an increasing plastic strain $\bar{\varepsilon}_m^p$, i.e.

$$E_0^s = \frac{1}{\frac{1}{E_0} + \frac{\bar{\varepsilon}_m^p}{\bar{\sigma}_m}} \tag{1}$$

where E_0 is the Young's modulus of the undeformed matrix. The effective stress and plastic strain are calculated as:

$$\bar{\sigma}_m = \sqrt{\frac{3}{2}\sigma'_{0_{ij}}\sigma'_{0_{ij}}},$$

$$\bar{\varepsilon}_m^p = \sqrt{\frac{2}{3}\varepsilon^p_{0_{ij}}\varepsilon^p_{0_{ij}}},$$

where $\sigma'_{0_{ij}}$ is the deviatoric stress. Accordingly, the secant shear modulus μ_0^s and secant Poisson's ratio v_0^s are found to be

$$\mu_0^s = \frac{E_0^s}{2(1+\nu_0^s)},$$

$$\nu_0^s = \frac{1}{2} - \left(\frac{1}{2} - \nu_0\right)\frac{E_0^s}{E_0},$$

where ν_0 is the initial Poisson's ratio and the last equation is derived from the condition of plastic incompressibility. Here and in the sequel, matrix, fibre and rubber particles or glass beads are denoted by "0", "1" and "2" respectively. Based on the von Mises yield criterion, the associated flow rule and a rate dependent strain hardening rule, the relationship between representative stress and strain after onset of yielding is assumed to be in a Cowper–Symonds (Symonds, 1967) form:

$$\bar{\sigma}_m = (\sigma_0 + H(\bar{\varepsilon}_m^p)^n)\left[1 + \left(\frac{\dot{\bar{\varepsilon}}_m^p}{D}\right)^{1/p}\right]. \tag{2}$$

This is an empirical equation that has been shown to fit many experimental results. It includes a strain hardening term (in curved brackets) and an overstress model of visco-plasticity (in square brackets). H, D, n and p may be regarded as purely empirical constants. In fact, to date many mathematical material models have been developed to describe the overstress and other rate dependent properties (Harding, 1989). None of these models is, however, generic enough and each has its limitations in accuracies and ranges of application. The object of this paper is not to determine the most adequate material model for the simulation but to characterize the effective macro-behaviour based on the interaction at the micro-scale. Therefore, rather than going into molecular details usually characterized by intermolecular free energy barriers in thermodynamics terms, the theory here simply utilizes a phenomenological constitutive equation. The various parameters are directly drawn from our compressive tests. Hence the strength differential effect pertaining to polymers is not taken into account. As for the deformation of composites, the most intuitive controlling variable might be the total strain rate. This is not the best choice for a theoretical internal rate variable. For an increment of applied loading, there corresponds an increment of elastic strain, which occurs instantaneously, and an increment of plastic strain, which needs time to develop. Since the time dependency of the plastic strain is a property of the material response to external load, the plastic strain rate serves as an internal variable in eqn (2).

The approach is basically an iteration process with a fully implicit time scheme (Xia, 1990): (1) at each time step, the plastic strain (or plastic strain increment) and hence the strain rate of the matrix are assumed; (2) the secant modulus of the matrix is then calculated; (3) the various stresses, strain disturbances and transformation strains (including both elastic and plastic components) can then be obtained; (4) the total stress on the yield locus is obtained based on the matrix stress and strain disturbances; (5) the calculated matrix effective stress is compared with the stress obtained directly from the constitutive equation using the assumed plastic strain and hence the plastic strain rate in step (1). If the error between the effective matrix stress and the flow stress lies below a tolerance, say 10^{-6}, the iteration terminates.

The Mori-Tanaka method bases the analysis on two systems, one is a reference model which is a pure matrix under the same external load as the second system which is a hybrid. The reference model embodies a stress $\bar{\sigma}$ and a strain $\bar{\varepsilon}$ due to the applied load. Under a prescribed impact velocity v_0, the far-field composite strain in the impact direction equals $\bar{\varepsilon}_{33}$ (being $-\ln(1-v_0 t/h_0)$, t is time and h_0 is a nominal specimen thickness). The composite strains in directions 11 and 22 will be evaluated later. Similarly, under a prescribed stress or free stress condition in, say direction 11 or 22, the composite stress in that direction will be $\bar{\sigma}_{11}$ or $\bar{\sigma}_{22}$ and the composite stress in direction 33 will be calculated later.

The average stress and strain of the matrix will differ from the stress and strain of the reference model by, $\tilde{\sigma}$ and $\tilde{\varepsilon}$. These are due to the introduction of second and third phases within the matrix. They are:

$$\varepsilon_0 = \bar{\varepsilon}+\tilde{\varepsilon},$$

$$\sigma_0 = \bar{\sigma}+\tilde{\sigma} = C_0^s(\bar{\varepsilon}+\tilde{\varepsilon}).$$

The average stress and strain of the fibres further differ from those of the surrounding matrix by an additional amount σ^1 and ε^1 and are given by,

$$\sigma_1 = \bar{\sigma}+\tilde{\sigma}+\sigma^1 = C_1(\bar{\varepsilon}+\tilde{\varepsilon}+\varepsilon^1) = C_0^s(\bar{\varepsilon}+\tilde{\varepsilon}+\varepsilon^1-\varepsilon^{*1}), \tag{3}$$

where C_0^s and C_1 are the secant modulus tensor, modulus tensor of the matrix and fibre respectively. The fibre perturbed strain ε^1 is related to the transformation strain ε^{*1} by

$$\varepsilon^1 = S_1\varepsilon^{*1},$$

where S_1 is the Eshelby tensor, dependent solely on the inclusion geometry and the secant Poisson's ratio of the matrix. Detailed expressions of the tensor for ellipsoidal inclusions are listed in the Appendix.

Now, for the second inclusion, namely either spherical rubber particles or spherical glass beads (denoted by "2"), the average stress and strain can be derived in the same way as for the first inclusion:

$$\sigma_2 = \bar{\sigma}+\tilde{\sigma}+\sigma^2 = C_2(\bar{\varepsilon}+\tilde{\varepsilon}+\varepsilon^2) = C_0^s(\bar{\varepsilon}+\tilde{\varepsilon}+\varepsilon^2-\varepsilon^{*2}). \tag{4}$$

The perturbed strain for the second inclusion ε^2 is related to the transformation strain ε^{*2} by the Eshelby tensors for spherical inhomogeneities:

$$\varepsilon^2 = S_2\varepsilon^{*2}.$$

So long as the polymer is under uniaxial compression, the only non-zero terms in stress and strain tensors are in the 11, 22 and 33 directions. No shear stress or strain exist. The prescribed displacement is applied in direction 33 whereas the overall zero stress condition must be satisfied laterally (in directions 11 and 22). Transverse isotropy is maintained. Namely, all strain components in direction 11 equal the corresponding strain components in direction 22. Equations (3) and (4) can be simplified to

$$\begin{aligned} C_{11}^i\varepsilon_{11}^{*i}+C_{12}^i\varepsilon_{33}^{*i} &= -2D_1^i(\bar{\varepsilon}_{11}+\tilde{\varepsilon}_{11})-(\bar{\varepsilon}_{33}+\tilde{\varepsilon}_{33}),\\ C_{21}^i\varepsilon_{11}^{*i}+C_{22}^i\varepsilon_{33}^{*i} &= -2(\bar{\varepsilon}_{11}+\tilde{\varepsilon}_{11})-D_2^i(\bar{\varepsilon}_{33}+\tilde{\varepsilon}_{33}), \end{aligned} \tag{5}$$

where

$$C_{11}^i = 2D_1^i(S_{1111}^i+S_{1122}^i)+\frac{2(\lambda_0+\mu_0)}{\lambda_i-\lambda_0}+2S_{3311}^i,$$

$$C_{12}^i = 2D_1^iS_{1133}^i+S_{3333}^i+\frac{\lambda_0}{\lambda_i-\lambda_0},$$

$$C_{21}^i = 2(S_{1111}^i+S_{1122}^i)+2D_2^iS_{3311}^i+\frac{2\lambda_0}{\lambda_i-\lambda_0},$$

$$C_{22}^i = 2S_{1133}^i+D_2S_{3333}^i+\frac{\lambda_0+2\mu_0}{\lambda_i-\lambda_0},$$

$$D_1^i = 1+\frac{\mu_i-\mu_0}{\lambda_i-\lambda_0},$$

$$D_2^i = 1+\frac{2(\mu_i-\mu_0)}{\lambda_i-\lambda_0}.$$

Here $i = 1$ represents fibre inclusion and $i = 2$ represents spherical inclusions such as rubber particles or glass beads. S^i are tensors for fibre inclusions ($i = 1$) and glass beads or rubber particles ($i = 2$) and λ_i and μ_i are Lamé constants. λ_0 and μ_0 are constants derived from the matrix secant modulus and secant Poisson's ratio. Solving eqn (5) for ε^*, we get:

$$\varepsilon_{11}^{*i} = \frac{B_1^i}{A^i}\bar{\varepsilon}_{11} + \frac{B_2^i}{A^i}\bar{\varepsilon}_{33} + \frac{B_2^i\bar{\varepsilon}_{33} + B_1^i\bar{\varepsilon}_{11}}{A^i},$$

$$\varepsilon_{33}^{*i} = \frac{B_3^i}{A^i}\bar{\varepsilon}_{11} + \frac{B_4^i}{A^i}\bar{\varepsilon}_{33} + \frac{B_4^i\bar{\varepsilon}_{33} + B_3^i\bar{\varepsilon}_{11}}{A^i},$$

where

$$A^i = C_{11}^i C_{22}^i - C_{21}^i C_{12}^i,$$
$$B_1^i = 2(C_{12}^i - D_1^i C_{22}^i),$$
$$B_2^i = D_2^i C_{12}^i - C_{22}^i,$$
$$B_3^i = 2(D_1^i C_{21}^i - C_{11}^i),$$
$$B_1^i = C_{21}^i - D_2^i C_{11}^i.$$

Furthermore, in view of the fact that $\bar{\varepsilon} = \sum_0^2 f_i\varepsilon_i$, one has

$$\bar{\varepsilon} = -f_1\varepsilon^1 - f_2\varepsilon^2,$$

where $f_i (i = 0, 2)$ are volume fractions of the matrix, fibres and spherical particles respectively. The above expression involves two equations with three unknowns $\bar{\varepsilon}_{11}$, $\bar{\varepsilon}_{33}$ and $\bar{\varepsilon}_{11}$. They must be solved in conjunction with a third equation which is the lateral free stress condition $\bar{\sigma}_{11} = 0 = \sum_0^2 f_i\sigma_{i_{11}}$ ($f_0 = 1 - f_1 - f_2$). This eventually leads to a system of algebraic equations:

$$A_{k1}\bar{\varepsilon}_{11} + A_{k2}\bar{\varepsilon}_{33} + A_{k3}\bar{\varepsilon}_{11} = P_k (k = 1, 3),$$

where

$$A_{11} = 1 + \sum_1^2 f_i\left[(S_{1111}^i + S_{1122}^i)\frac{B_1^i}{A^i} + S_{1133}^i\frac{B_3^i}{A^i}\right],$$

$$A_{12} = \sum_1^2 f_i\left[(S_{1111}^i + S_{1122}^i)\frac{B_2^i}{A^i} + S_{1133}^i\frac{B_4^i}{A^i}\right],$$

$$A_{13} = \sum_1^2 f_i\left[(S_{1111}^i + S_{1122}^i)\frac{B_1^i}{A^i} + S_{1133}^i\frac{B_3^i}{A^i}\right],$$

$$P_1 = -\sum_1^2 f_i\left[(S_{1111}^i + S_{1122}^i)\frac{B_2^i}{A^i} + S_{1133}^i\frac{B_4^i}{A^i}\right]\bar{\varepsilon}_{33},$$

$$A_{21} = \sum_1^2 f_i\left[(S_{3311}^i + S_{3322}^i)\frac{B_1^i}{A^i} + S_{3333}^i\frac{B_3^i}{A^i}\right],$$

$$A_{22} = 1 + \sum_1^2 f_i\left[(S_{3311}^i + S_{3322}^i)\frac{B_2^i}{A^i} + S_{3333}^i\frac{B_4^i}{A^i}\right],$$

$$P_2 = -\sum_1^2 f_i\left[(S_{3311}^i + S_{3322}^i)\frac{B_2^i}{A^i} + S_{3333}^i\frac{B_4^i}{A^i}\right]\bar{\varepsilon}_{33},$$

$$A_{31} = \sum_0^2 f_i(2\lambda_i + 2\mu_i) + \sum_1^2 f_i(2\lambda_i + 2\mu_i)\left[(S^i_{1111} + S^i_{1122})\frac{B^i_1}{A^i} + S^i_{1133}\frac{B^i_3}{A^i}\right]$$
$$+ \sum_1^2 f_i\lambda_i\left[(S^i_{3311} + S^i_{3322})\frac{B^i_1}{A^i} + S^i_{3333}\frac{B^i_3}{A^i}\right],$$

$$A_{32} = \sum_0^2 f_i\lambda_i + \sum_1^2 f_i(2\lambda_i + 2\mu_i)\left[(S^i_{1111} + S^i_{1122})\frac{B^i_2}{A^i + S^i_{1133}\dfrac{B^i_4}{A^i}}\right]$$
$$+ \sum_1^2 f_i\lambda_i\left[(S^i_{3311} + S^i_{3322})\frac{B^i_2}{A^i} + S^i_{3333}\frac{B^i_4}{A^i}\right],$$

$$A_{33} = A_{31},$$

$$P_3 = -\sum_0^2 f_i\lambda_i\bar{\varepsilon}_{33} - \sum_1^2 f_i(2\lambda_i + 2\mu_i)\left[(S^i_{1111} + S^i_{1122})\frac{B^i_2}{A^i} + S^i_{1133}\frac{B^i_4}{A^i}\right]\bar{\varepsilon}_{33}$$
$$- \sum_1^2 f_i\lambda_i\left[(S^i_{3311} + S^i_{3322})\frac{B^i_2}{A^i} + S^i_{3333}\frac{B^i_4}{A^i}\right]\bar{\varepsilon}_{33}.$$

Once the transformation strains and perturbed strains are obtained, stresses and strains of different phases can be subsequently worked out.

3. RESPONSE OF THE COMPOSITES

Before proceeding with any calculation, the constants in the matrix constitutive relation must be decided based on some experimental results. They are: $\sigma_0 = 55$ MPa, $H = 7.69$ MPa, $n = 1$, $D = 350\ \text{s}^{-1}$ and $p = 5.5$. The material elastic properties are: $E_0 = 2.5$ GPa and $\nu_0 = 0.42$ for undeformed matrix, $E = 72$ GPa and $\nu = 0.3$ for glass and $E = 50$ MPa, $\nu = 0.4999$ for rubber. The specimen nominal thickness h_0 is 8 mm. To achieve material response for at least three decades of strain rate, loading velocity is assumed to vary between 0.01 and 20 m s^{-1}.

3.1. *Effect of inclusion configurations*

A system consisting of matrix mixed with only one type of inclusion is considered first to highlight the interaction between the matrix and the inclusions. The effect of a pure inclusion can be best illustrated by evaluating the overall composite stress–strain curve under the same impact velocity. The configurations concerned are:

—pure glass fibre reinforcement (vertical and horizontal),
—pure glass bead reinforcement,
—pure rubber particle additives.

Figures 2–6 give curves for composite stresses vs composite strains with strains up to 10% for the various composites with only one phase of inclusions or simply pure matrix. In terms of overall performance, the strengths can be listed in a decreasing order as follows: longer vertical (in direction 33) fibre & matrix, short vertical fibre & matrix, longer horizontal (in direction 11 or 22) fibre & matrix, short horizontal fibre & matrix, pure bead & matrix, pure matrix, pure rubber particle & matrix. Here "longer fibre" means fibres having aspect ratio $\alpha = 15$ while "short fibres" have an aspect ratio of 5. It can also be seen that the volume fraction has a substantial influence on the initial linear proportionality of the curves and the apparent yield stresses. The overall plastic strain hardening effect draws from the elasticity of the inclusions and the strain and strain rate hardening of the matrix. No specific particle size is explicitly accounted for here due to the fact that it will not appreciably alter the modulus at constant volume fraction (Moloney *et al.*, 1987), provided that these inclusions are well bonded. In contrast, the aspect ratio will largely alter the

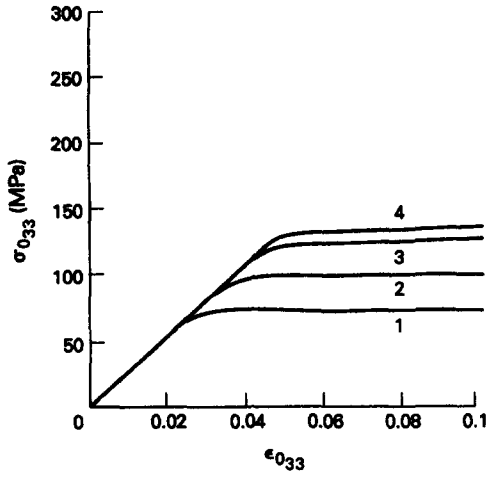

Fig. 2. Stresses vs strains for pure matrix. (1) $v_0 = 0.01$ m s^{-1}. (2) $v_0 = 1$ m s^{-1}. (3) $v_0 = 10$ m s^{-1}. (4) $v_0 = 20$ m s^{-1}.

behaviour of fibre reinforced composites. The longer the fibres ($\alpha = 15$), the higher the strength of composites in compression. It is believed that as fibre length increases, failure modes would alter from fibre movement to fibre failure. Hence, just like under tension, there might be a length beyond which the overall compressive strength drops. This is beyond the scope of current work.

The analysis might be elaborated further by considering matrix mixed with three-dimensional array of fibres. Observation after impact tests, however, show that nearly all short fibres rotate to a position vertical to the impact direction. That prompts us to look at the two extreme cases where fibres are either aligned parallel or perpendicular to the loading direction, albeit the fact that it is not difficult to model a composite with random arrays of fibre (Qiu and Weng, 1991). Apparently, composites with fibres lying in direction 33 are stronger than cases when fibres lie in direction 11 or 22. This is because to deform a composite globally, fibres lying in direction 33 will have to be deformed with the composite while pure matrix deformation dominates the composite deformation if fibres are arranged in direction 11 or 22.

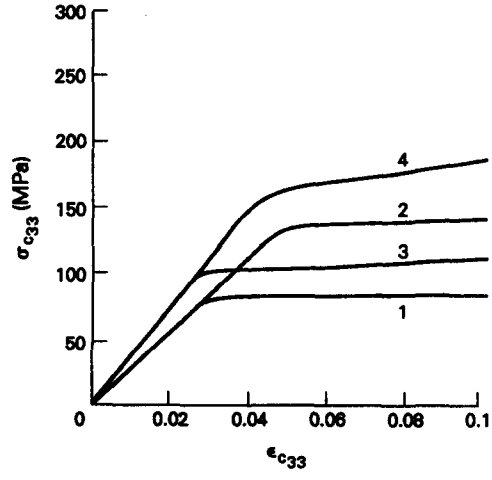

Fig. 3. Composite overall stresses vs overall strains. Materials: horizontally aligned glass fibres, matrix. (1) $f_1 = 5\%$, $\alpha = 5$, $v_0 = 0.01$ m s^{-1}. (2) $f_1 = 5\%$, $\alpha = 5$, $v_0 = 10$ m s^{-1}. (3) $f_1 = 20\%$, $\alpha = 5$, $v_0 = 0.01$ m s^{-1}. (4) $f_1 = 20\%$, $\alpha = 5$, $v_0 = 10$ m s^{-1}.

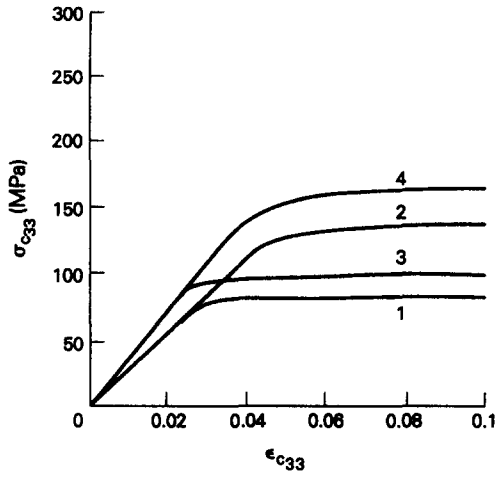

Fig. 4. Composite overall stresses vs overall strains. Materials: spherical glass beads, matrix. (1) $f_2 = 5\%$, $v_0 = 0.01$ m s^{-1}. (2) $f_2 = 5\%$, $v_0 = 10$ m s^{-1}. (3) $f_2 = 20\%$, $v_0 = 0.01$ m s^{-1}. (4) $f_2 = 20\%$, $v_0 = 10$ m s^{-1}.

Now that our aim is to achieve high resistance with low material damage, it is not sufficient to confine attention only to overall composite stress–strain curves. The matrix stress or strain is another important indicator of material response, bearing in mind that the composite stress and strain are the weighted sum of its constituents. Subsequently, for a composite strain of 0.05, the matrix would undergo a strain exceeding 0.05 if the inclusion is a harder phase, or below 0.05 if the inclusion is a softer phase. Also seen from the figures is the fact that, under controlled displacement impact, a harder inclusion will inflict higher strain, higher plastic strain rate and eventually a higher stress in the matrix. In Fig. 7, clearly the matrix is subject to the largest deformation and load when fibre volume fraction is 20%. Conversely, when mixed with pure rubber, the matrix will be the least loaded compared with pure matrix, at the expense of overall resistance.

Having studied the effect of single type inclusions and the corresponding matrix stress, a hybrid composite, i.e. a mixture of short fibres, rubber particulates and resin matrix may be made, to achieve high overall strength without large matrix stresses. Figure 8 gives the composite overall stress-overall strain for this type of hybrid with fibres of 5% and rubbers of 20% volume fractions.

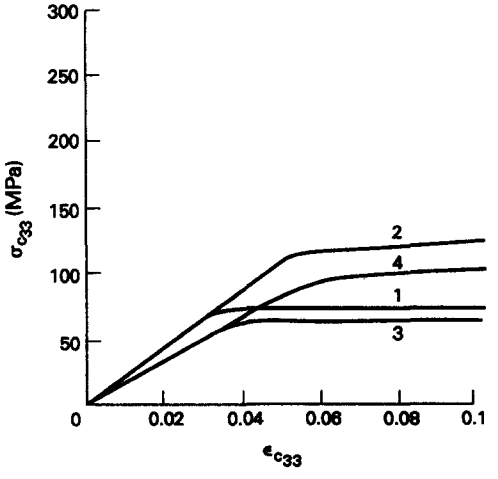

Fig. 5. Composite overall stresses vs overall strains. Materials: rubber spheres, matrix. (1) $f_2 = 5\%$, $v_0 = 0.01$ m s^{-1}. (2) $f_2 = 5\%$, $v_0 = 10$ m s^{-1}. (3) $f_2 = 20\%$, $v_0 = 0.01$ m s^{-1}. (4) $f_2 = 20\%$, $v_0 = 10$ m s^{-1}.

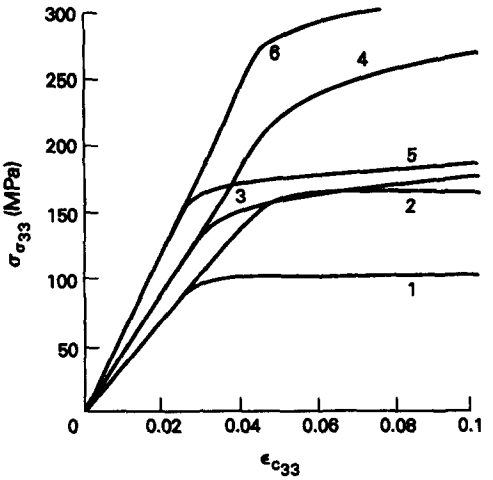

Fig. 6. Composite overall stresses vs overall strains. Materials: vertically aligned glass fibres, matrix. (1) $f_1 = 5\%$, $\alpha = 5$, $v_0 = 0.01$ m s^{-1}. (2) $f_1 = 5\%$, $\alpha = 5$, $v_0 = 10$ m s^{-1}. (3) $f_1 = 5\%$, $\alpha = 15$, $v_0 = 0.01$ m s^{-1}. (4) $f_1 = 5\%$, $\alpha = 15$, $v_0 = 10$ m s^{-1}. (5) $f_1 = 20\%$, $\alpha = 5$, $v_0 = 0.01$ m s^{-1}. (6) $f_1 = 20\%$, $\alpha = 5$, $v_0 = 10$ m s^{-1}.

For a hybrid with 5% fibre and 20% rubber, Fig. 7 shows that the matrix stress and final strain, are reduced compared with pure fibre as inclusion or pure matrix without inclusions. The overall composite stress and strain curve now lies between fibre mono-composites and pure matrix, by comparing curve 2 of Fig. 8 with curve 2 of Fig. 2 and curve 3 of Fig. 6. Of course by adjusting the contents of each constituent, say reducing the rubber contents from 20% to 10%, the 5% fibre+10% rubber composite will produce higher effective modulus with smaller increase in matrix stress. The evaluation of stresses of composite and stresses of matrix must be a relative measure of their own strengths.

A rubber phase will reduce the strain of the resin as deformation will be concentrated within the rubber phase. This tends to reduce the stress inside the resin (see Fig. 7). On the other hand, a fibre inclusion will cause high matrix stress and strain due to misfit in properties and deformation. The two phenomena counteract in the composites. Another effect which does not show up prominently in the current uniaxial stress state is the constraint offered by matrix to rubber particle which is virtually incompressible. The

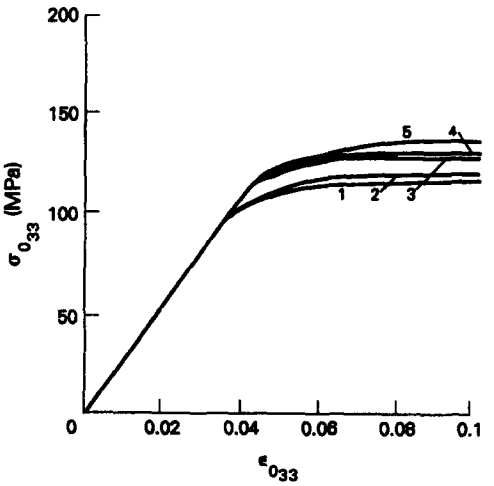

Fig. 7. Matrix stresses vs matrix strains, $v_0 = 10$ m s^{-1}. (1) 20% rubber spheres+matrix. (2) 5% vertically aligned short ($\alpha = 5$) glass fibres+20% rubber spheres+matrix. (3) Pure matrix. (4) 5% vertically aligned short ($\alpha = 5$) glass fibres+matrix. (5) 20% vertically aligned short ($\alpha = 5$) glass fibres+matrix.

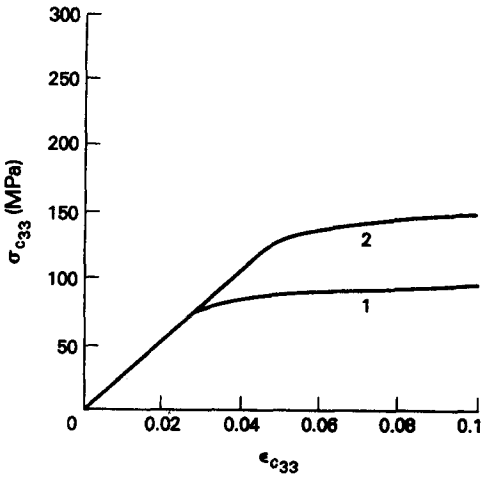

Fig. 8. Composite overall stresses vs overall strains. Materials: vertically aligned glass fibres ($\alpha = 5$), rubber spheres, matrix. (1) $f_1 = 5\%$, $f_2 = 20\%$, $v_0 = 0.01$ m s^{-1}. (2) $f_1 = 5\%$, $f_2 = 20\%$, $v_0 = 10$ m s^{-1}.

constraint, though always weakening due to matrix plastic deformation, will induce volumetric stress onto the rubber particles. The quasi-hydrostatic pressure thus generated will have some effect on the overall resistance, especially if the matrix itself is constrained laterally and the rubber volume fraction is high.

3.2. *Effect of strain rate*

The strain rate effect here means viscoplastic response of the matrix and the rate dependent constraining power of the matrix to inclusions at the micro-scale. This ends up with rate dependency of the overall composite.

The enhancement of the apparent yielding stress of the overall composites can be found directly from Figs 3–8 when the impact velocity increases from 0.01 to 1 m s^{-1}, to 10 m s^{-1} and finally to 20 m s^{-1}. The resulting calculated plastic strain rates of the matrix thus span three decades from 10^{-1} to 10^3 s^{-1}.

The plastic strain rate for the matrix against total matrix strain for hybrid composites under 10 m s^{-1} constant velocity impact is shown in Fig. 9. Strain rate shoots up at the

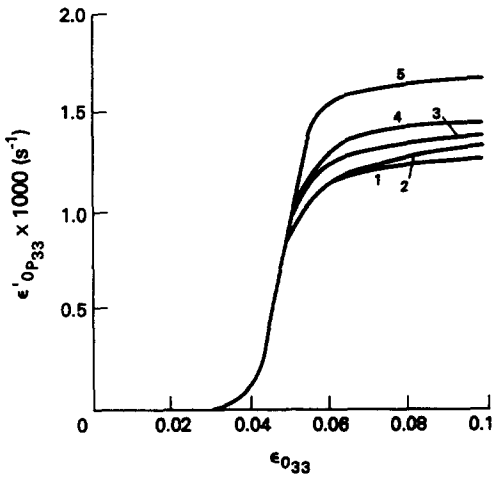

Fig. 9. Matrix plastic strain rates vs matrix strain ($v_0 = 10$ m s^{-1}). (1) 20% rubber spheres+matrix. (2) 5% vertically aligned glass fibres ($\alpha = 5$)+20% rubber spheres+matrix. (3) Pure matrix. (4) 5% vertically aligned glass fibres ($\alpha = 5$)+matrix. (5) 20% vertically aligned glass fibres ($\alpha = 5$)+matrix.

very beginning to about 1300 s^{-1} when plastic deformation commences and then changes its pattern to gradual increase. The value of matrix plastic strain rate depends on the type, the volume fraction and the configuration of inclusions. The interaction between fibre phase and matrix leads to higher rates of matrix strain at fibre volume fraction of 5% and even higher when the volume fraction further increases to 20%. In cases of 5% fibre and 20% rubber hybrid composites, the matrix plastic strain rate is less than for the pure matrix but later it increases and edges near that of the pure matrix. Even so, the matrix stress for the hybrid (curve 2 of Fig. 7) still lies below the stress for the pure matrix. Therefore, it seems that rubber and fibre hybrids will reduce the matrix stress significantly but not the matrix strain rate when comparing curve 2 with 3 in Fig. 7 and curve 2 with 3 in Fig. 9. The reason why the not-so-much reduced strain rate does not harden the matrix is the fact that the interaction of rubber particles and fibres with matrix is an instantaneous response while the rate effect takes time to build up.

Many publications have appeared [for instance, Yee and Pearson (1989)] in areas of strain rate effect on rubber modified epoxy under tension and of rubber toughening mechanisms. Nevertheless, for compressive loading at high rates, the work on hybrids remains few. Here we confine the study to rate effect on rubber modified polymer under monotonic compression. Further work on rate dependent failure mode is required, though work on transient failure of unidirectional composites (Xia and Ruiz, 1991, 1992) and adhesively bonded laminates (Ruiz and Xia, 1991) have been done. No comparison of the results here with any other works is given. The analytical work, though qualitatively correlated with our experimental results (Xia *et al.*, 1991), cannot be accurately recaptured from our much idealized finite element results as it is computationally impossible to disperse any large quantities of discrete phases within a matrix by the finite element method.

4. CONCLUSIONS

This paper highlights the theoretical part of an investigation on fibre and rubber modified epoxy. Based on a micro-mechanical model in conjunction with an empirical constitutive equation for the matrix, the rate dependent interaction among different phases: fibres, beads, particles and resins, is illustrated.

The overall strength of a composite is directly linked to the aspect ratio, volume fraction, alignment of inclusions, with fibres of high volume fraction, large aspect ratio and in line with the loading direction offering the highest overall reaction force. However, the rate dependent but weakening constraining power of the matrix is strongly influenced by the configuration of the inclusions, with high volume fraction, large aspect ratio and fibres lying along the direction of load inducing the largest matrix strain and strain rate and hence constraining power to the inclusion. In order to have a polymer with strong resistance but small matrix deformation, the concept of mixing polymers is thus proposed. This is proved to be a compromising if not a synergic mechanism within the initial loading stage of interest here, on top of the fact that rubber particles would greatly toughen the thermoset resin if further unloading and failure start to occur.

Acknowledgements—This work is partly funded by a SERC grant and partly funded by RARDE, U.K. The author thanks Dr C. Ruiz, director of the University Technology Centre, Oxford, for his support and encouragement.

REFERENCES

Christensen, R. M. (1990). A critical evaluation for a class of micro-mechanics models. *J. Mech. Phys. Solids* **38**(3), 379–404.

Harding, J. (1989). The development of constitutive relationships for material behaviour at high rates of strain. In *Fourth Int. Conf. Mech. Prop. Materials at High Rates of Strain, Oxford* (Edited by J. Harding), pp. 189–203.

Moloney, A. C., Kausch, H. H., Kaiser, T. and Beer, H. R. (1987). Review: parameters determining the strength and toughness of particulate filled epoxide resins. *J. Mater. Sci.* **22**(2), 381–393.

Qiu, Y. P. and Weng, G. J. (1991). The influence of inclusion shape on the overall elastoplastic behaviour of a two phase isotropic composite. *Int. J. Solids Structures* **27**(12), 1537–1550.

Ruiz, C. and Xia, Y. (1991). Significance of the interlaminar strength of composites under impact loading. In *Composite Materials Symposium, Houston, TX* (Edited by D. Hui and T. J. Kozik), pp. 161–166.
Symonds, P. S. (1967). Survey of methods of analysis for plastic deformation of structures under dynamic loading. Div. Engineering Report, Brown University.
Tandon, G. P. and Weng, G. J. (1988). A theory of particle reinforced plasticity. *J. Appl. Mech.* **55**(1), 126–135.
Taya, M. and Arsenault, R. (1989). *Metal Matrix Composites: Thermomechanical Behavior*. Pergamon Press, Oxford.
Taya, M. and Chou, T. W. (1981). On the two kinds of ellipsoidal inhomogeneities in an infinite elastic body: an application to a hybrid composite. *Int. J. Solids Structures* **17**(6), 553–563.
Weng, G. J. (1988). Theoretical principles for the determination of two kinds of composite plasticity: inclusions plastic vs matrix plastic. In *Mechanics of Composite Materials* (Edited by G. J. Dvorak and N. Laws), AMD-Vol. 92, pp. 193–208. ASME, New York.
Withers, P. J., Stobbs, W. M. and Pedersen, O. B. (1989). The application of the Eshelby method of internal stress determination to short fibre metal composites. *Acta Metall.* **37**(11), 3061–3084.
Xia, Y. (1990). Dynamic Application of ABAQUS. Oxford University Report, OUEL 1853/90, also presented at U.K. ABAQUS training course, Manchester, 1990.
Xia, Y. and Ruiz, C. (1991). Analysis of damage in stress wave loaded unidirectional composites. *Comput. Struct.* **38**(3), 251–258.
Xia, Y. and Ruiz, C. (1992). A transient stochastic failure model for unidirectional composites under impact loading. *Compos. Sci. Tech.* **43**(1), 25–36.
Xia, Y., Ruiz, C. and Harding, J. (1991). Dynamic compression of adhesive materials. RARDE, MoD (unpublished).
Yee, A. F. and Pearson, R. A. (1989). Fractography and failure mechanisms of rubber modified epoxide resins. In *Fractography and Failure Mechanisms of Polymers and Composites* (Edited by A. Roulin-Moloney), pp. 291–350. Elsevier Applied Science, London.

APPENDIX

Eshelby's tensors S_{ijkl} for isotropic matrix are a function of the geometry of ellipsoid with axes a_1, a_2 and a_3 and secant Poisson's ratio of the matrix v. a_1, a_2 and a_3 are the principal axes of an ellipsoid.

For an oblate spheroid: $a_1 = a_2 > a_3$:

$$S_{1111} = S_{2222} = \frac{3}{8(1-v)}\frac{\alpha^2}{(\alpha^2-1)} + \frac{1}{4(1-v)}\left[1-2v-\frac{9}{4(\alpha^2-1)}\right]g,$$

$$S_{3333} = \frac{1}{2(1-v)}\left\{1-2v+\frac{(3\alpha^2-1)}{(\alpha^2-1)} - \left[1-2v+\frac{3\alpha^2}{(\alpha^2-1)}\right]g\right\},$$

$$S_{1122} = S_{2211} = \frac{1}{4(1-v)}\left\{\frac{\alpha^2}{2(\alpha^2-1)} - \left[(1-2v)+\frac{3}{4(\alpha^2-1)}\right]g\right\},$$

$$S_{1133} = S_{2233} = -\frac{1}{2(1-v)}\frac{\alpha^2}{(\alpha^2-1)} + \frac{1}{4(1-v)}\left[\frac{3\alpha^2}{(\alpha^2-1)} - (1-2v)\right]g,$$

$$S_{3311} = S_{3322} = -\frac{1}{2(1-v)}\left[1-2v+\frac{1}{(\alpha^2-1)}\right] + \frac{1}{2(1-v)}\left[1-2v+\frac{3}{2(\alpha^2-1)}\right]g,$$

$$g = \frac{\alpha}{(\alpha^2-1)^{3/2}}[\alpha(\alpha^2-1)^{1/2} - \cosh^{-1}\alpha](\alpha = l/d).$$

For a prolate spheroid: $a_1 = a_2 < a_3$:

$$S_{1111} = S_{2222} = -\frac{3}{8(1-v)}\frac{\alpha^2}{(1-\alpha^2)} + \frac{1}{4(1-v)}\left[1-2v+\frac{9}{4(1-\alpha^2)}\right]g,$$

$$S_{3333} = \frac{1}{2(1-v)}\left\{4-2v-\frac{2}{(1-\alpha^2)}\right] + \frac{1}{2(1-v)}\left[-4+2v+\frac{3}{(1-\alpha^2)}\right]g\right\},$$

$$S_{1122} = S_{2211} = \frac{1}{8(1-v)}\left[1-\frac{1}{(1-\alpha^2)}\right] + \frac{1}{16(1-v)}\left[-4(1-2v)+\frac{3}{(1-\alpha^2)}\right]g,$$

$$S_{1133} = S_{2233} = \frac{1}{2(1-v)}\frac{\alpha^2}{(1-\alpha^2)} - \frac{1}{4(1-v)}\left[1-2v+\frac{3\alpha^2}{(1-\alpha^2)}\right]g,$$

$$S_{3311} = S_{3322} = \frac{1}{2(1-v)}\left[-1+2v+\frac{1}{(1-\alpha^2)}\right] + \frac{1}{4(1-v)}\left[2(1-2v)-\frac{3}{(1-\alpha^2)}\right]g,$$

$$g = \frac{\alpha}{(1-\alpha^2)^{3/2}}[\cos^{-1}\alpha - \alpha(1-\alpha^2)^{1/2}](\alpha = l/d).$$

For a sphere: $a_1 = a_2 = a_3$:

$$S_{1111} = S_{2222} = S_{3333} = \frac{7-5\nu}{15(1-\nu)},$$

$$S_{1122} = S_{2233} = S_{3311} = S_{1133} = S_{2211} = S_{3322} = \frac{5\nu-1}{15(1-\nu)}.$$